ELSEVIER

Ceramics International 26 (2000) 583–587

CERAMICS INTERNATIONAL

Investigations of co-existence region in lead zirconate-titanate solid solutions: X-ray diffraction studies

Ahmed Boutarfaia

Institut des Sciences Exactes, Université de Biskra, BP 145, RP-Biskra (07000), Algeria

Received 23 April 1998; accepted 3 July 1998

Abstract

Compositions with varying Zr/Ti ratio in: xPbZrO$_3$–yPbTiO$_3$–zPb(Fe$_{1/5}$, Ni$_{1/5}$, Sb$_{3/5}$)O$_3$ such that $(x+y+z)=100\%$ and at constant $z=10\%$ were prepared by the conventional method of thermal synthesis of mixed-oxides. The characterization of these PZT ceramics was carried out with XRD and SEM. X-ray diffraction is presented to demonstrate the co-existence of the tetragonal and rhombohedral phases. In the present work it is shown that the tetragonal structure persists up to $x=43$, while the rhombohedral structure appears at $x=46$. These results suggest that the morphotropic phase boundary lies in the range $43<x<46$ and therefore the width of the morphotropic transition is determined ($\Delta x=3\%$). The lattice parameter measurements showed that tetragonal and rhombohedral unit cells of the phases depend on the sintering temperature. The effects of sintering temperature on microstructure are studied by means of a scanning electron microscope (SEM).

Keywords: A. Sintering; B. Microstructure; B. X-ray methods; D. PZT; Co-existence of phases in PZT

1. Introduction

In ceramic manufacturing technology, piezoelectric PZT ceramic compositions are most likely to be near the morphotropic phase boundary [1]. The electromechanical response of these ceramics is known to be most pronounced at the morphotropic phase boundary (MPB) composition which separates the tetragonal (Ti rich) and rhombohedral (Zr rich) phase fields. Despite extensive work on the location of the MPB, considerable controversy exists about the nature and exact composition range of the MPB [2–8].

In the practical applications of PZT, various impurities have been added in order to improve the piezoelectric properties. Some researchers investigated the effect of small amounts of impurities on the dielectric and piezoelectric properties of perovskite materials. Other variants of the sintering process are concerned with achieving dense microstructures of homogenous grain size. Porosity and grain have a significant effect on the piezoelectric properties of the sintered ceramics [5]. Also, it is interesting to observe the influence of the calcination and heat treatment conditions on the density, which increases with increasing temperature and time [6].

Investigations of the Pb(Zr$_x$, Ti$_{1-x}$)O$_3$ system have shown the existence of an almost temperature-independent morphotropic phase boundary at $x=0.535$, which separates a rhombohedral phase from a tetragonal one. By means of X-ray diffraction, the co-existence of the two phases over a range of compositions around MPB was demonstrated [7–14]. Many authors have suggested the existence of a range of compositions where both the tetragonal and rhombohedral phases are thermodynamically stable [7–8].

The influence of technological factors on the width of the co-existence region was investigated on the ternary system PbZrO$_3$–PbTiO$_3$–Pb(Fe$_{1/5}$, Ni$_{1/5}$, Sb$_{3/5}$)O$_3$ by X-ray diffraction, because this system is likely to provide a narrow width.

The present paper reports the influence of sintering temperature on density, porosity and grain size on the ceramic. The purpose of the investigation is to determine the width of co-existence of tetragonal and rhombohedral phases and the exact composition of the MPB

0272-8842/00/$ - see front matter
PII: S0272-8842(99)00099-1

in chemically homogeneous PZT powders made by the classic ceramic technique.

2. Experimental

The composition used in this experiment was as follows: xPbZrO$_3$–yPbTiO$_3$–zPb(Fe$_{1/5}$, Ni$_{1/5}$, Sb$_{3/5}$)O$_3$, where $x+y+z=100\%$, $39 < x < 47$, $43 < y < 51$, $z=10\%$ (constant). This chemical formula is abbreviated in the text as PZT–PFNS. In this study the samples were prepared from pure oxides Pb_3O_4, TiO_2, ZrO_2, Fe_2O_3, NiO, Sb_2O_3, dried at 120°C for 3 to 4 h. The chemical purity of each was >99%.

A mixture of the starting powders were was milled and mixed in a vibratory mill, wet homogenized with distilled water for 6 h and pressed at 10 000 kg/cm^2 into pellets. The samples for analysis after reaction were fired at the required temperature for 2 h in covered alumina crucibles at the following temperature: 850, 950, 1050, 1150 and 1180°C. The sintering process was conducted in a lead-rich environment to minimize lead volatilization. After sintering, the samples experienced ≈2% weight loss. The samples were pale yellow after sintering and remained this color throughout processing. Densities of sintered pieces were measured from the samples dimensions and weights, i.e the density of 44PbZrO$_3$–46PbTiO$_3$–10Pb(Fe$_{1/5}$, Ni$_{1/5}$, Sb$_{3/5}$)O$_3$ ceramic samples sintered at 1150°C was 7.72×10^3 kg/m^3.

The calcined and sintered samples were characterized for second-phase formation by means of a Siemens D500 diffractometer, operated at 40 kV and 30 mA, using CuK_α radiation with a nickel filter. The compositions of the PZT phases were identified by an analysis of the peaks [002 (tetragonal), 200 (tetragonal), 200 (rhombohedral)] in the 2θ range 43–46°. The tetragonal, rhombohedral and tetragonal–rhombohedral phases were characterized and their lattice parameters were calculated. In order to ensure an accurate determination of the lattice parameters, the X-ray peaks were recorded gradually with 0.01° steps.

Scanning electron micrographs (SEM) were taken from fractured as well as chemically etched surfaces. A section of the sintered sample was etched in a 5% HCl solution for 3 min. The fractured surfaces were used for grain size and morphology determination. The size distribution of the grains was measured and the results compared with each other. The size distribution of the pores and the total value of porosity were determined on a polished cross-section of the samples with an image analyzer.

3. Results and discussion

Fig. 1(a) represents the density of sintered 44PbZrO$_3$–46PbTiO$_3$–10Pb(Fe$_{1/5}$, Ni$_{1/5}$, Sb$_{3/5}$)O$_3$ samples as a function of temperature. The density increases in the initial period with sintering temperature and saturates beyond 1150°C. From these results, the optimum firing temperature for the maximum density, ρ, of the ceramic is between 1050 and 1180°C. At 1150°C, 97% of the theoretical value was achieved. Sintering at 1180°C caused the density to decrease. The optimum value of the sintering temperature was affected by the additions of impurities and other processing parameters, such as the rate of heating, time of thermal treatment, and composition of the protecting atmosphere. The optimum sintering temperature was taken as the point when the PbO vapor pressure evaporation–recondensation equilibrium for the reaction: PbO−PbO (vapor)−Pb (vapor) + 1/2 O_2 was established [14]. Increase of the porosity for temperatures higher than the optimum can, therefore, be attributed to a greater rate of evaporation of PbO compared to that recondensed.

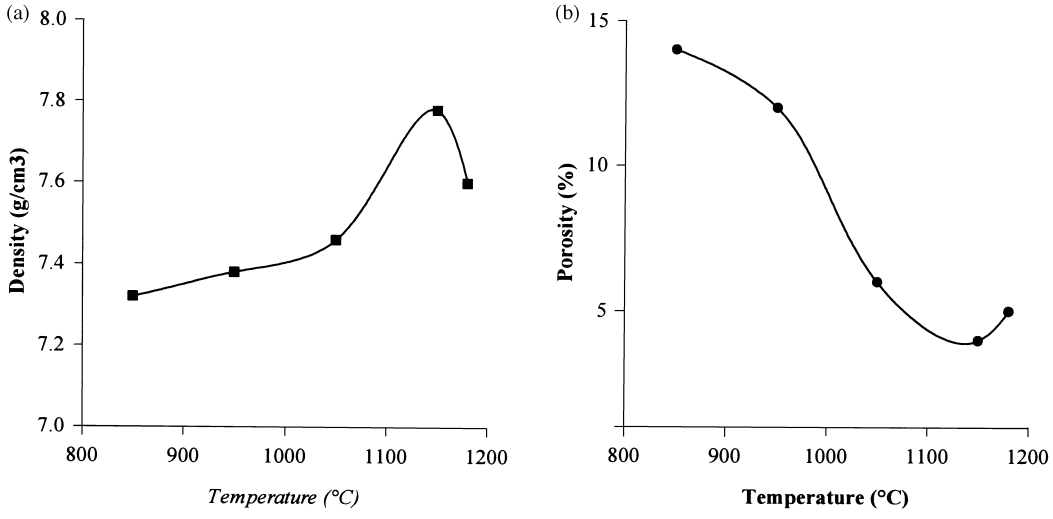

Fig. 1. Density and porosity versus sintering temperature for 44PbZrO$_3$–46PbTiO$_3$–10Pb(Fe$_{1/5}$, Ni$_{1/5}$, Sb$_{3/5}$)O$_3$ ceramics (sintering time 2 h).

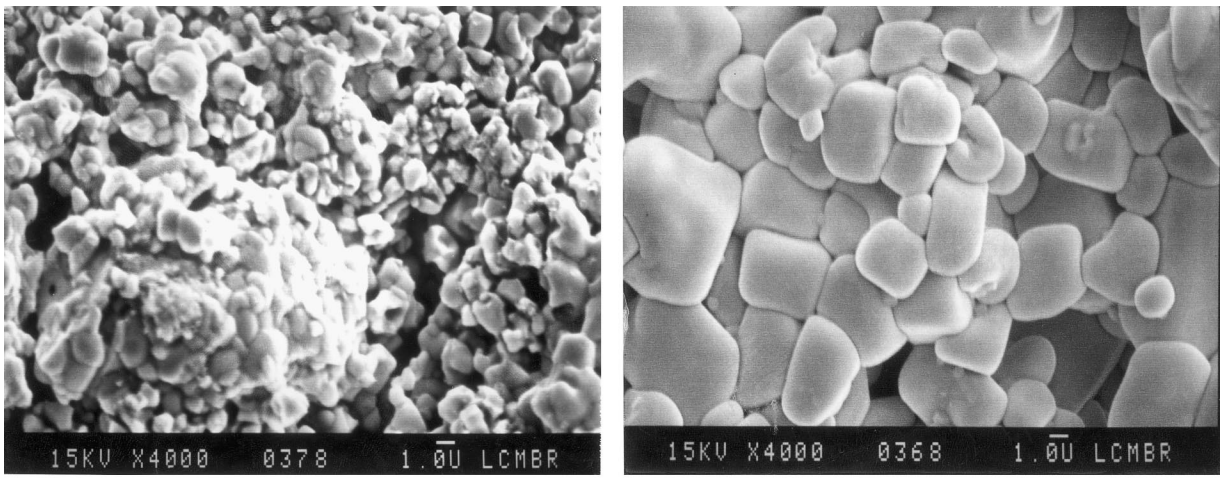

(a) (b)

Fig. 2. Scanning electron micrographs of polished and chemically etched cross-sections of 44 $PbZrO_3$–46$PbTiO_3$–10$Pb(Fe_{1/5}, Ni_{1/5}, Sb_{3/5})O_3$ sintered at 850 and 1150°C.

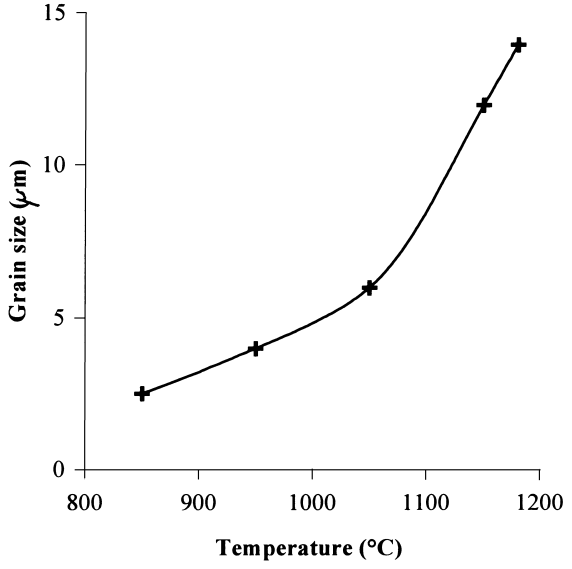

Fig. 3. Grain size versus sintering temperature for 44$PbZrO_3$–46$PbTiO_3$–10$Pb(Fe_{1/5}, Ni_{1/5}, Sb_{3/5})O_3$ ceramics (sintering time 2 h).

Table 1
Series of compositions and crystal structure

Compositions	Crystal structure[a]				
x/*y*/*z*	850°C	950°C	1050°C	1150°C	1180°C
A_1:47/43/10	R	R	R	R	R
A_2:46/44/10	T + R	T + R	R	R	R
A_3:45/45/10	T + R	T + R	T + R	T + R	T + R
A_4:44/46/10	T + R	T + R	T + R	T + R	T + R
A_5:43/47/10	T + R	T + R	T + R	T	T
A_6:41/49/10	T + R	T	T		
A_7:39/51/10	T				

[a] T = tetragonal; R = rhombohedral; T + R = tetragonal–rhombohedral.

Additions of different oxides to PZT-type ceramics influence the densification and the grain size. The process involves a decrease in the number and size of the pores together with an increase in the grain sizes. The porosity, determined by means of the image analyzer as a function of sintering temperature, is given in Fig. 1(b). Addition of $Pb(Fe_{1/5}, Ni_{1/5}, Sb_{3/5})O_3$ (10%) caused an increase in densification rate and the inhibition of grain growth. From the data it can be noticed that the peak value of the density corresponds to the lowest value of porosity at 1150°C. Fig. 2(a) and (b) shows scanning electron micrographs of the specimens sintered at 850 and 1150°C, respectively. From these images, it can be deduced that the decrease of porosity with increasing sintering temperature, is due to a decrease in the number and size of the pores. The variation of porosity as a function of sintering temperature shows a greater densification rate for doped samples with respect to previous results in which pore diameters averaged 4 to 14 μm [15].

SEM photographs of PZT–PFNS composition and Fig. 3 describe the microstructural evolution. Grain size increases with increasing sintering temperature. A uniform microstructure was obtained at 1150°C while the average grain size was 12–14 μm. This was caused by the coexistence of the two phases in these materials. Small crystallites occur in the samples sintered at 850°C with dimensions similar to those of the initial powder. At lower sintering temperature (950°C), the average grain diameters have practically the same values (1–2 μm) as those at 850°C, but at higher temperatures (1050–1180°C), (10–12 or 12–14 μm) are encountered.

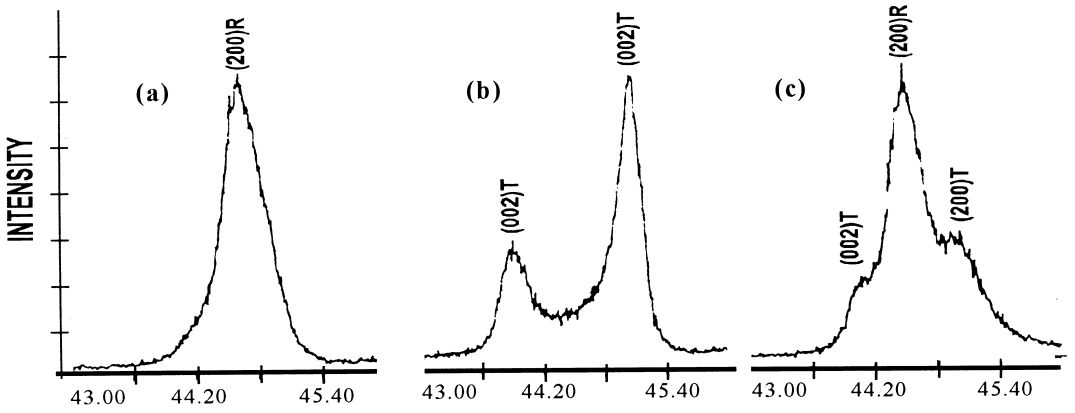

Fig. 4. XRD patterns obtained xPbZrO$_3$–yPbTiO$_3$–10Pb(Fe, Ni, Sb)O$_3$ after crushing the pellets at 1150°C for 2 h: (a) x/y:46/44; (b) x/y:43/47; (c) x/y:44/46. The co-existence of tetragonal and rhombohedral splitting in the (c).

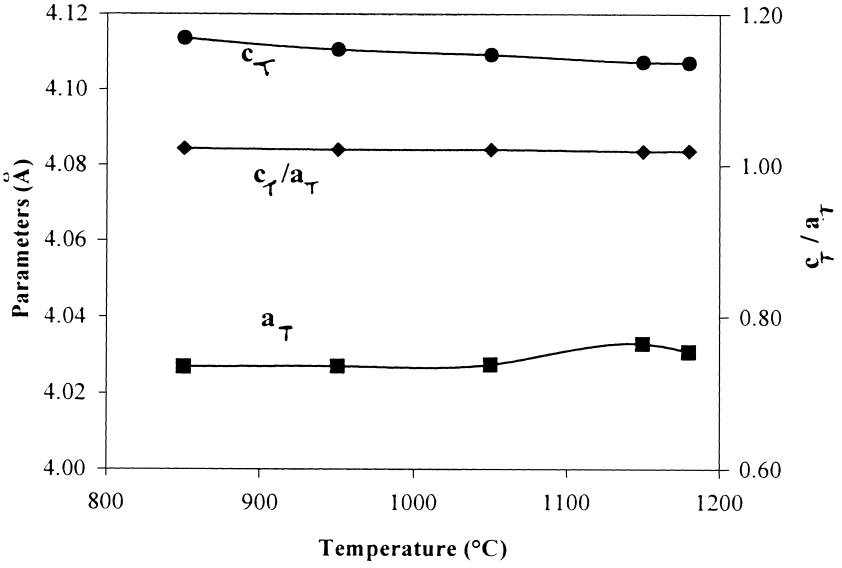

Fig. 5. Lattice constant variations for both coexisting ferroelectric phases as a function of sintering temperature.

Sintered powders were examined by X-ray diffractometry to ensure phase purity and to identify the phases and lattice constants of the materials. The co-existence of tetragonal and rhombohedral phases near the morphotropic phase boundary implies the existence of compositional fluctuations. The compositional fluctuation can in principle be determined from the width of the X-ray diffraction peaks. However, determination of the compositional fluctuation for samples near the morphotropic phase boundary is difficult. XRD patterns of PZT powders were analyzed to detect the characteristic rhombohedral and tetragonal splitting. A morphotropic phase boundary "co-existence region" was observed [shown by duplicated (200) peaks]. It has been reported in the literature that the splitting of these reflections into triplets takes place in conventionally-prepared ceramics due to compositional fluctuations leading to the co-existence of the tetragonal and rhombohedral phases (T + R).

The X-ray diffraction patterns of: xPbZrO$_3$–yPbTiO$_3$–zPb(Fe$_{1/5}$, Ni$_{1/5}$, Sb$_{3/5}$)O$_3$ materials (x = 39–47), represented by samples A$_1$...A$_7$, are given in Table 1. The typical XRD pattern of PZT–PFNS sample sintered at 1150°C is given in Fig. 4. Triplet peaks around $2\theta = 45°$ indicate that the specimen consists of a mixture of tetragonal and rhombohedral phases. The reflections marked ***T*** are assigned to tetragonal phase, whereas those with ***R*** are assigned to rhombohedral phase: transition from rhombohedral to tetragonal phase is observed as the concentration of PbTiO$_3$ increases. Throughout this transition is a region where both

phases exist simultaneously. At 1150°C, It is shown that the tetragonal structure can be formed up to $x_T < 44$ while the rhombohedral structure becomes stabilized for $x_R > 45$. However, at $x = 44$–45, tetragonal and rhombohedral phases co-exist. The co-existence region is therefore quite narrow ($\Delta x \approx 0.03$) and extends between x_T and x_R. The width $\Delta x = x_T - x_R$ of the co-existence region from our work is close to that obtained by others [4,8,10]. Δx varies with temperature; the higher the temperature, the lower the value of Δx.

Compositions near the morphotropic phase boundary also were investigated. In this region, the lattice constants are very sensitive to composition. Using (002) and (200) diffraction lines of the tetragonal, c_T and a_T phase and the (200) line of the rhombohedral, a_R, phase, lattice constants were determined using the (220) diffraction line of Si (99.9%) powder as an internal standard. Lattice parameters and tetragonal distortion for $44PbZrO_3$–$46PbTiO_3$–$10Pb(Fe_{1/5}, Ni_{1/5}, Sb_{3/5})O_3$ ceramics are calculated from XRD patterns and plotted in Fig. 5. The relative error in measuring the parameters was $\Delta a/a = \Delta c/c = 0.002$ Å. The variation of the lattice parameters as a function of sintering temperature could be explained by the enhancement of cation diffusion. and consequently by the homogenization of the microcomposition.

The variation in the lattice parameters of the identified phase composition shows that the values of th c_T/a_T ratio have decreased. This can be explained by microscopic compositional fluctuations occurring in these perovskite materials, which cannot provide a real homogeneity in the solid solutions, which determine the co-existence of tetragonal–rhombohedral phases. The increase of sintering temperature and firing time enhanced the diffusion effects within these regions and led to a relative homogenization of the local composition in the material. The transition from tetragonal to rhombohedral phase as a function of composition can be visualized to occur as follows:

- The tetragonal and rhombohedral distortions decrease continuously as one approaches the MPB composition from either side.
- If the tetragonal to rhombohedral transition is first order the two phases might coexist over some range of x around the MPB composition.

4. Conclusions

The effect of sintering temperature on the density and grain size of PZT–PFNS ceramics has been investigated. It was demonstrated that the grain size increased continuously with sintering temperature. Increase of the porosity for temperatures higher than the optimum can, therefore, be obtained to a greater rate evaporation of PbO compared to that recondensed. Microstructural studies of PZT–PFNS, obtained at different sintering in the 850 to 1180°C range, have shown the existence of the minimum porosity at a determined optimum sintering temperature.

The phase of the sintered samples were examined by X-ray diffractometry (XRD). In this work, the solid solution $xPbZrO_3$–$yPbTiO_3$–$zPb(Fe_{1/5}, Ni_{1/5}, Sb_{3/5})O_3$ are studied. The morphotropic phase boundary (MPB) of solid solution is located at $x = 44$–45. It was found that the MPB is not a narrow and vertically straight boundary but a region whose width depends on the firing temperature.

The lattice parameters a_T and c_T of the tetragonal structure and a_R the rhombohedral structure were found to vary with sintering temperature.

References

[1] B. Jaffe, W.R. Cook, H. Jaffe, Piezoelectric Ceramics, Academic Press, London/New York, 1971.
[2] K. Karl, K.H. Hardtl, Phys. Stat. Sol. 8 (1971) 87.
[3] A. Pinczuk, Solid State Communn. 12 (1973) 1035.
[4] V.A. Isupov, Solid State Communn. 17 (1975) 1331.
[5] K. Okazaki, K. Nagata, J. Am. Ceram. Soc. 56 (1973) 82.
[6] D.A. Buckner, P.D. Wilcox, Am. Ceram. Soc. Bull. 52 (1972) 218.
[7] K. Kakegawa, J. Mohri, K. Takahashi, H. Yamamura, S. Shirasaki, Solid State Commun. 24 (1977) 769.
[8] P. Ari-Gur, L. Benguigui, Solid State Commun. 15 (1974) 1077.
[9] P. Ari-Gur, L. Benguigui, J. Phys. D. 8 (1975) 1856.
[10] A. Boutarfaia, C. Boudaren, A. Mousser, S.E. Bouaoud, Ceramics International 21 (1995) 391.
[11] A. Boutarfaia, S.E. Bouaoud, Ceramics International 22 (1996) 282.
[12] S.A. Mabud, J. Appl. Cryst. 13 (1980) 211.
[13] Y. Kala, Phys. Status Solidi A 78 (1983) 277.
[14] R.B. Atkin, R.M. Fulrath, J. Am. Ceram. Soc. 54 (5) (1971) 265.
[15] R.B. Atkin, R.M. Holman, R.M. Fulrath, J. Am. Ceram. Soc. 54 (2) (1971) 113.